Preparation and Properties of Poly(lactide-co-glycolide) (PLGA)/ Nano-Hydroxyapatite (NHA) Scaffolds by Thermally Induced Phase Separation and Rabbit MSCs Culture on Scaffolds

Y.X. Huang, J. Ren, C. Chen, T.B. Ren, X.Y. Zhou

Preparation and Properties of Poly(lactide-co-glycolide) (PLGA)/ Nano-Hydroxyapatite (NHA) Scaffolds by Thermally Induced Phase Separation and Rabbit MSCs Culture on Scaffolds

Y. X. HUANG,[1] J. REN,[1,2,*] C. CHEN,[1] T. B. REN[1] AND X. Y. ZHOU[1]
[1]*Institute of Nano and Bio-Polymeric Materials and* [2]*Key Laboratory Advanced Civil Engineering Materials, Ministry of Education School of Material Science and Engineering, TongJi University Shanghai 200092, P.R. China*

ABSTRACT: Biodegradable polymer/bioceramic composites scaffold can overcome the limitation of conventional ceramic bone substitutes such as brittleness and difficulty in shaping. To better mimic the mineral component and the microstructure of natural bone, novel nano-hydroxyapatite (NHA)/polymer composite scaffolds with high porosity and well-controlled pore architectures as well as high exposure of the bioactive ceramics to the scaffold surface is developed for efficient bone tissue engineering. In this article, regular and highly interconnected porous poly(lactide-co-glycolide) (PLGA)/NHA scaffolds are fabricated by thermally induced phase separation technique. The effects of solvent composition, polymer concentration, coarsening temperature, and coarsening time as well as NHA content on the micro-morphology, mechanical properties of the PLGA/NHA scaffolds are investigated. The results show that pore size of the PLGA/NHA scaffolds decrease with the increase of PLGA concentration and NHA content. The introduction of NHA greatly increase the mechanical properties and water absorption ability which greatly increase with the increase of NHA content. Mesenchymal stem cells are seeded and cultured in

*Author to whom correspondence should be addressed.
E-mail: renjie@mail.tongji.edu.cn
Figure 12 appears in color online: http://jba.sagepub.com

0885-3282/08/05 0409–24 $10.00/0 DOI: 10.1177/0885328207077632

three-dimensional (3D) PLGA/NHA scaffolds to fabricate *in vitro* tissue engineering bone, which is investigated by adhesion rate, cell morphology, cell numbers, and alkaline phosphatase assay. The results display that the PLGA/NHA scaffolds exhibit significantly higher cell growth, alkaline phosphatase activity than PLGA scaffolds, especially the PLGA/NHA scaffolds with 10 wt.% NHA. The results suggest that the newly developed PLGA/NHA composite scaffolds may serve as an excellent 3D substrate for cell attachment and migration in bone tissue engineering.

KEY WORDS: poly(lactide-co-glycolide), nano-hydroxyapatite, thermally induced phase separation, scaffold, mesenchymal stem cells.

INTRODUCTION

In the tissue engineering approach, the temporary three-dimensional (3D) scaffold serves an important role in the manipulation of the functions of osteoblasts and a central role in the guidance of new bone formation into desired shapes. In principle, a biodegradable matrix with sufficient mechanical strength, optimized architecture and suitable degradation rate, which could finally be replaced by newly formed bone, is most desirable. Over the past decade, the main goal of bone tissue engineering has been to develop biodegradable materials as bone graft substitutes for filling large bone defects [1–3].

Hydroxyapatite (HA) is a bioactive, biocompatible, osteoconductive and osteoinductive ceramic material [4]. Its biocompatibility is thought to be due to its chemical and structural similarity to the mineral phase of native bone [5]. However, its clinical applications have been limited because of its brittleness, difficulty of shaping [6], and an extremely slow degradation rate [7]. In addition, HA has poor mechanical properties and the newly formed bone in a porous HA network cannot sustain the mechanical loading needed for remodeling [6]. Recent research also suggests that better osteoconductivity would be achieved if synthetic HA could resemble bone mineral more in composition, size, and morphology [8,9]. In addition, nano-sized HA may have other special properties due to its small size and huge specific surface area. Webster et al. [10,11] have shown significant increase in protein adsorption and osteoblast adhesion on the nano-sized ceramic materials compared to traditional micro-sized ceramic materials.

Biodegradable polyesters such as poly(lactic acid) (PLA), poly(glycolic acid) (PGA), and their copolymers (PLGA), have been widely used for the preparation of 3D scaffolds for bone tissue engineering application because of their good biocompatibility and biodegradability as well as the innocuity of their degradation products. Although all these materials

have been approved by Food and Drug Administration (FDA), most of them are poor in cell affinity which limits their application in tissue engineering [12,13] and are too flexible and too weak to meet the mechanical strength requirement [14–16]. Moreover, the acidic substance from their degradation could accelerate their degradation in return, and hence induce inflammatory reactions [17,18]. To combine the osteoconductivity of calcium phosphates and good biodegradability of polyesters, polymer/ceramic composite scaffolds have been developed for bone tissue engineering either by direct mixing or by a biomimetic approach [19–21]. Compared to plain polymer scaffolds in which neo tissue matrix was formed only in surface layer ($<240\,\mu m$) [22], the composite scaffolds supported cells, growth and neo tissue formation throughout the scaffold including in the very center of the scaffold [23].

Over the past few years, many methods of preparation of scaffolds, such as porogen leaching [24–26], gas expansion [27], and emulsion drying [28], have been reported. Recently, a new method of freeze-drying via thermally induced phase separation (TIPS) was developed and received great attention in industrial applications for the preparation of polyester scaffolds [29,30].

In this article, porous poly(lactide-co-glycolide) (PLGA/Nano-hydroxyapatite) (NHA) scaffolds would be fabricated by TIPS technique, and the effect of solvent composition, polymer concentration, coarsening time, and temperature as well as NHA content on the microstructure and properties of scaffolds were investigated. Rabbit mesenchymal stem cells (MSCs) were seeded and cultured in 3D PLGA/NHA scaffolds to fabricate *in vitro* tissue engineering bone, which was studied by adhesion rate, cell morphology, cell numbers, and alkaline phosphatase (ALP) assay.

MATERIALS AND METHODS

Materials

Poly(D,L-lactic-co-glycolic acid) (PLGA) (72/28), $M_w = 165$, 920, $PI = 1.82$, and NHA powder, $D_n = 96\,nm$, was provided by our lab. 1,4-dioxane, analytical quality, was provided by National Pharmaceutical Group Co. (China). The water used was twice-distilled deionized water.

Cloud-point Temperature Measurements

The cloud-point temperature of a polymer solution depends on the solvent and composition. In this article, the solvent was a mixture of distilled water and 1,4-dioxane with the volume ratio of 87/13 or 85/15.

The cloud point was measured as described in the following: the cloud-point temperatures of the PLGA/1,4-dioxane/water ternary systems were determined by visual turbidimetry. PLGA was dissolved in a 1,4-dioxane/water mixture in various concentration (2, 4, 6, 8, and 10 wt.%) with a magnetic stirrer by heating at 60°C for 2 h. The sample was then maintained as a clear solution at a temperature ca. 15°C above the expected cloud-point temperature. This solution was then slowly cooled in steps of 1°C, equilibrating the system for 10 min at each new temperature. The cloud-point temperature was considered as the temperature at which the clear PLGA solution turned to be turbid visually as determined by visual inspection. The error range was approximately ±1°C.

Preparation of Scaffolds

The preparation of scaffolds can be divided into two parts. The first one is about the determination of the cloud-point temperature of the polymer solution. The second one is about the preparation of the scaffolds.

Figure 1 is the process of TIPS technique for PLGA/NHA scaffold preparation. First, NHA powders were dispersed in 1,4-dioxane/water mixture by ultrasonication. Second, PLGA was added into the solution when the NHA powders have been dispersed in the mixture uniformly. Third, the PLGA/NHA compounds were heated at 65°C in the ultrasonator until the mixed solution turned into homogeneous PLGA/NHA solution. Then the tube of dissolved sample was heated to 15°C above the measured cloud-point temperature, after which it was quickly dipped into a constant temperature bath maintained at the desired quenching temperature (5 or 9°C). The tube was removed from the quenching bath after (0.5, 2, 4, 6 or 8 h) to observe the coarsening effect. The annealed sample was immediately immersed in liquid nitrogen to be fast frozen. At last, the sample was freeze-dried at −60°C and 14 Pa for at least 48 h to remove the solvents, yielding the porous scaffolds.

Characterization of Scaffolds

Morphology Characterization

The porous morphology of the PLGA/NHA scaffolds was investigated by scanning electron microscopy (SEM, Hitachi S-2360N). Fracture-frozen cross sections of the scaffold, taken either in a longitudinal or transverse way, were coated with gold and observed under SEM at an accelerating voltage of 20 KV.

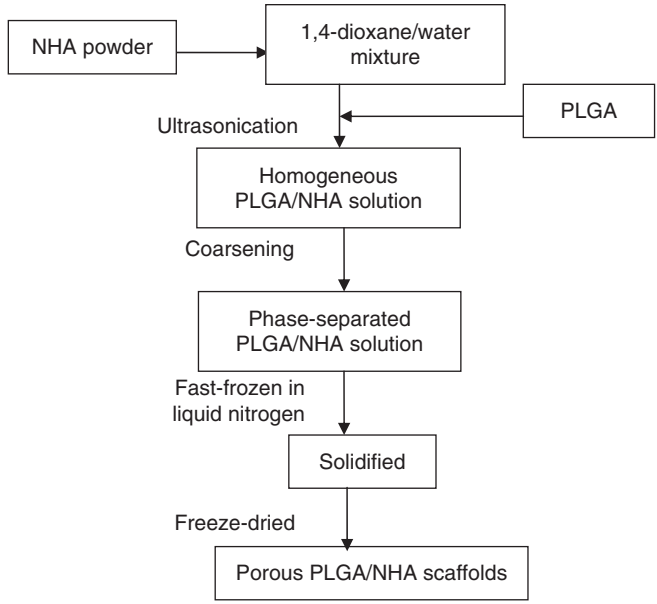

Figure 1. The preparation of PLGA/NHA scaffold by TIPS.

Porosity

The porosity of the PLGA/NHA scaffolds was measured by liquid displacement method. Absolute ethanol with density ρ was used as displacement liquid and operated at 25°C, because it can penetrate easily into the scaffolds and would not induce shrinkage or swelling as a nonsolvent of the PLGA. The samples, pycnometer and ethanol were kept at 25°C for 4 h before testing. A pycnometer filled full with ethanol was weighed, W_1. A scaffold sample of weight W_S was immersed into the bottle full of ethanol, and then the bottle was surged slowly until the air in the scaffold was all moved out. At last, the pycnometer was refilled with ethanol and was weighed, W_2. The scaffold saturated with ethanol was taken out of the pycnometer and then the pycnometer was weighed, W_3.

The volume of the scaffold sample is $V_s = (W_1 - W_2 + W_S)/\rho$, while the total volume of the pores in it is $V_p = (W_2 - W_3 - W_S)/\rho$. The porosity of the tested sample is

$$\varepsilon = \frac{V_p}{V_p + V_s} = \frac{W_2 - W_3 - W_S}{W_1 - W_3} \tag{1}$$

Mechanical Properties

The compression strength of scaffold was tested using a computer-controlled DXLL-5000 mechanical tester and a crosshead speed of 5 mm/min was used. Each sample has dimensions of 16 mm in diameter and 3 mm in thickness. Five specimens of each sample were tested and the average compression strength of the five specimens was the compression strength of the sample.

Water Absorption Ability

Samples weighed as W_1 were immersed and soaked in twice-distilled water, and were taken out to weigh as W_2 after 1, 2, 4, 8, 12 and 24 h. Then, the water absorption rate for samples at different times is $(W_2 - W_1)/W_1 \times 100\%$.

MSCs Culture and Cells Seeding

Seeding of Scaffolds

Rabbit MSCs were obtained from the tibia of an immature (2 months old) white New Zealand rabbit as described by Solchaga et al [31]. The MSCs were cultured in Dulbecco's modified Eagle's medium (DMEM) with 10% fetal bovine serum (FBS). Third-passage cells were used for the experiments.

The PLGA scaffolds ($10 \times 5 \times 5$ mm) were prewetted in a culture medium DMEM, Gibco for 24 h after being disinfected by ^{60}Co. The MSCs were suspended at the concentration of 1×10^7 cells/mL, and 0.1 mL of the cells suspension was poured onto each scaffold. The scaffolds were left undisturbed in an incubator for 3 h to allow the cells to attach to the scaffolds, and then the scaffolds were covered with 2 mL of media (DMEM). The cell/scaffold constructs were cultured in a humidified incubator at 37°C with 5% (v/v) CO_2 and the media was supplemented and changed every three days.

Cell Numbers

After cultured for different days, the specimens were taken out of the culture media and rinsed twice and then 0.7 mL assimilation liquid (0.25% trypsin and 0.02% EDTA) was put into the specimens to assimilate for 3–5 min. After assimilation ended using 0.1 mL FBS, the liquid in the specimens was squeezed out and the cells were counted by cells count board.

Alkaline Phosphatase Assay

The ALP production of osteoblasts cultured on scaffolds was measured spectroscopically ($n = 3$). The osteoblast/scaffold constructs seeded for 3, 7, 14 days were washed three times with PBS (1M, pH 7.4), and sonicated for 4 min on ice. Aliquots of 20 μL were incubated with 1 mL of a *p*-nitrophenyl phosphate solution (16 mM, Sigma) at 30°C for up to 5 min. The production of *p*-nitrophenol in the presence of ALP was measured by monitoring light absorbance at 410 nm.

Cell Morphology

The surface morphologies of cells/scaffold constructs were examined using a ESEM (EFEG-SEM, Quanta 200 FEG, FEI Company). The samples were washed twice with PBS, prefixed in 1% (v/v) buffered glutaraldehyde for 1 h, and fixed in 0.1% (v/v) buffered formaldehyde for 24 h. The fixed sample was observed in room temperature through ESEM.

Statistical Analysis

Quantitative data were expressed as the mean ± SD. Statistical comparisons were carried out using analysis of variance (ANOVA, SAS Institute Inc., Cary, NC, USA). A value of $p < 0.05$ was considered to be statistically significant.

RESULTS

The Phase Diagram of PLGA Solution

The cloud-point temperature of each PLGA/1,4-dioxane/water ternary systems was determined as the temperature at which a slowly cooled solution was visually judged to have become turbid, which seems to be induced by liquid–liquid demixing between solvent and nonsolvent.

Figure 2 shows the cloud-point/composition phase diagram of the PLGA/1,4-dioxane/water ternary system. The solvent/nonsolvent ratio were 87/13 and 85/15 by volume, respectively. For two of the ternary systems, the cloud-point temperatures increase slightly with increasing polymer concentration. The cloud-point temperature (~20°C) of the PLGA system is dramatically increased when the water content in the solvent mixture is increased. This indicates that liquid–liquid demixing depends mainly on the water content of the solvent mixture. Similar behavior has been observed by Hua et al. [32] research.

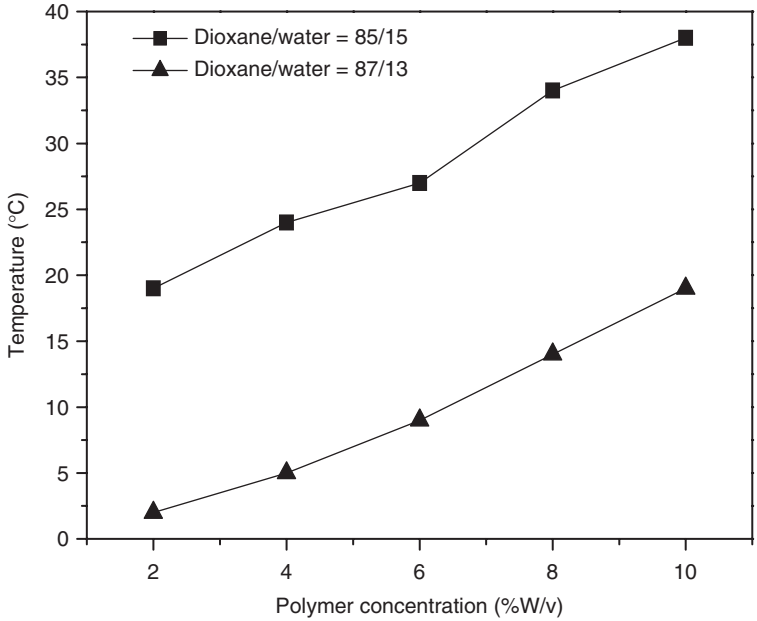

Figure 2. Phase diagram of cloud-point temperature vs polymer composition of the PLGA-1,4-dioxane-water ternary system.

It must be pointed that although Figure 2 shows the Phase diagram of cloud-point temperature versus polymer composition of the PLGA/1,4 dioxane/water ternary system, it also indicates the phase diagram of PLGA/NHA/1,4-dioxane/water quaternary system because NHA has very little influence on the cloud-point temperature.

Effect of Solvent Composition

Hua et al. [32] has reported that solvent composition strongly influenced scaffold morphology. To compare the effects of different solvents on the dispersing behavior of NHA powders and microstructure of the final products, PLGA/NHA (95/5) scaffolds from 10% (w/v) PLGA in the two kinds of 1,4-dioxane/water solvent mentioned earlier were prepared. Both of them were coarsened for 4 h at same quenching depth (the temperature difference between cloud-point and coarsening temperature) 10°C, i.e., 9°C for 1,4-dioxane/water 87/13 and 28°C for 85/15. The corresponding SEM is illustrated in Figure 3. Macroporous (>100 μm) scaffolds were obtained from both solutions, while the

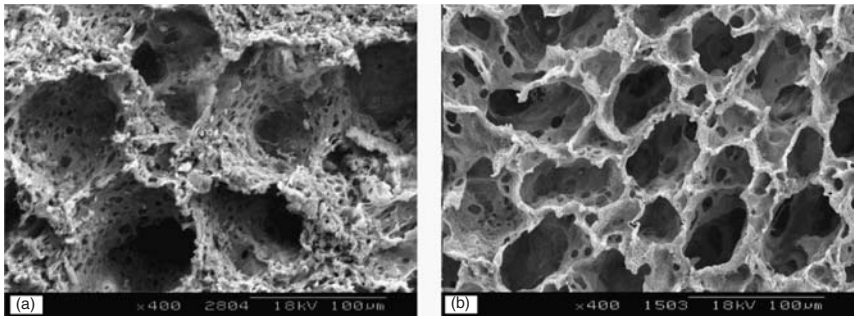

Figure 3. SEM micrographs of PLGA/NHA (95/5) scaffolds prepared from 10% (w/v) PLGA/dioxane/water mixtures with different solvent compositions (a) 1,4-dioxane/water, 85/15; (b) 1,4 –dioxane/water, 87/13.

scaffold from PLGA/NHA in 87/13 solvent is much more interconnected and regular than that from 85/15 solvent.

Effect of Polymer Concentration

The effect of polymer concentration in 1,4-dioxane/water (87/13) mixture on scaffold morphology was investigated by taking SEM images of the structure of the scaffolds from 8 and 10% (w/v) PLGA/dioxane/water mixtures. Both the PLGA solutions were coarsened at 5°C for 4 h, so the quenching depth of them are 9°C and 14°C, respectively. The SEM (Figure 4) shows they have different morphology. The pore structure of the former is much more uniform, with a lot of highly interconnected pores ranging from 50 to 200 μm. The small pores are settled in the big one and linked with each other. However, although the latter also contain many pores, most of the pores are too small (10–40 μm) and isolated with each other.

To verify whether the same phenomenon appears in PLGA/NHA system or not, PLGA/NHA (95/5 by weight) scaffolds were prepared from 8 and 10% (w/v) PLGA/NHA/dioxane/water mixtures solution. The solutions were also coarsened at 5°C (quenching depth are 9°C and 14°C, respectively) for 4 h and similar phenomenon was observed. Data plotted in Figure 5 shows the great difference between the microstructure of two composite scaffolds prepared. For the system with a lower polymer concentration (8%), open macro-pores (about 100 μm) are distributed in the whole sample uniformly, while the one prepared from higher polymer concentration (10%) seems like a rugged flat without any pores but with rough and irregular surface. Even though the high concentration of polymer solutions have larger driving force because of larger

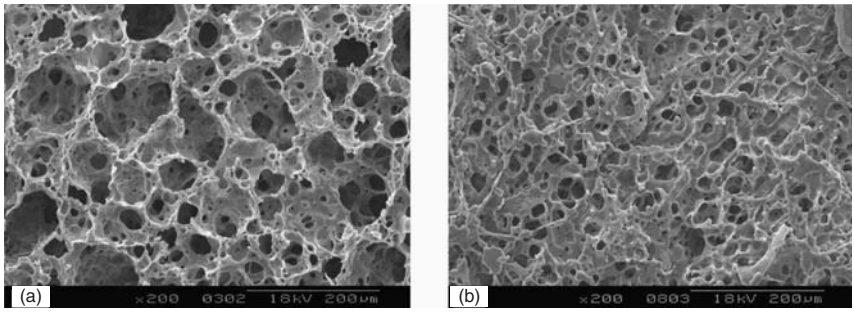

Figure 4. SEM micrographs of PLGA scaffolds prepared from PLGA/dioxane mixture (1,4-dioxane/water, 87/13) with different polymer concentrations at coarsening temperature of 5°C for 4 h: (a) 8% (w/v) PLGA/dioxane mixture and (b) 10% (w/v) PLGA/dioxane mixture.

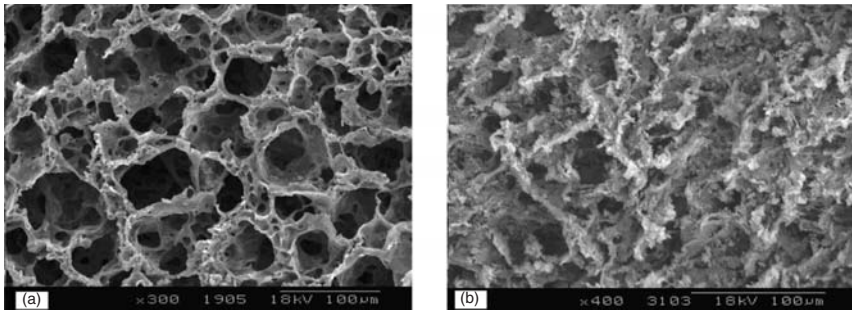

Figure 5. SEM micrographs of PLGA/NHA (PLGA/NHA: 95/5) scaffolds prepared from PLGA/NHA/dioxane mixture(1,4-dioxane/water, 87/13) with different polymer concentrations at coarsening temperature of 5°C for 4 h: (a) 8% (w/v) PLGA/dioxane mixture and (b) 10% (w/v) PLGA/dioxane mixture.

quenching depth for phase separation, the microstructure seems more irregular. This can be explained in terms of the prevention of phase separation due to the viscosity increase caused by high concentration of PLGA solution.

The porosity of the four scaffolds discussed previously is presented in Table 1. The porosity decreases with the increase of polymer concentration. The porosity was also greatly decreased because of introduction of NHA in polymer solution. These results are consistent with that of SEM images. Both of the scaffolds prepared from 8 wt.% PLGA solution have high porosity of >84%, which was helpful for cell's adhesion and proliferation.

Table 1. Porosity of the PLGA/NHA scaffolds prepared by TIPS method with different PLGA concentrations (SD ± 5%).

Composition	PLGA concentration (wt %)	Porosity (%)
PLGA/NHA: 100/0	8	91.1
PLGA/NHA: 100/0	10	79.2
PLGA/NHA: 95/5	8	84.2
PLGA/NHA: 95/5	10	63.1

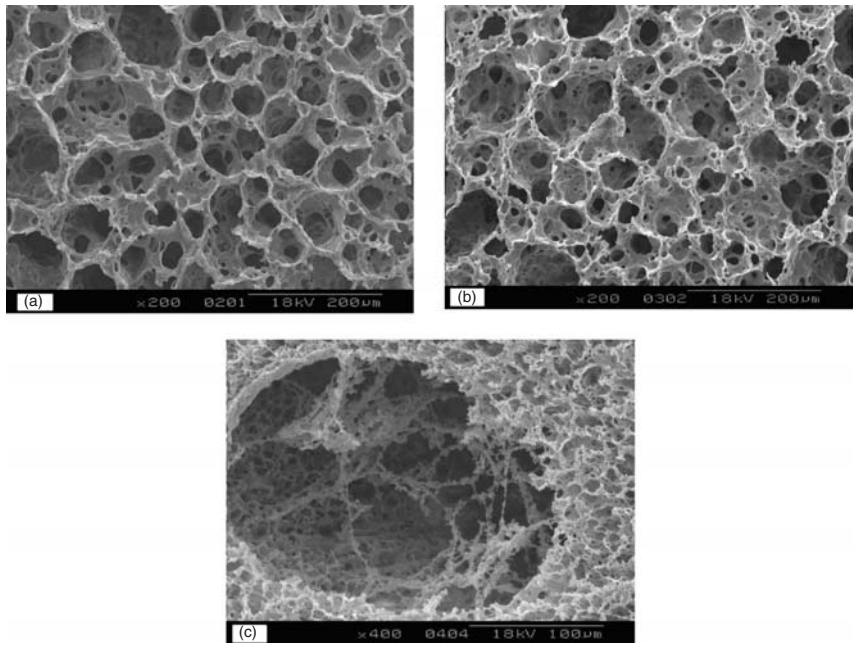

Figure 6. SEM images of PLGA scaffolds prepared from 8% (w/v) PLGA/dioxane/water mixtures (1,4-dioxane/water, 87/13) at different quenching time (a) 2 h; (b) 4 h; and (c) 8 h.

Effect of Quenching Time and Temperature

Quenching temperature and time have dominating effect on the final mircostructure of the scaffolds and play very important role in controlling scaffold formation [32]. Figure 6 illustrates SEM images of PLGA scaffolds from 8% (w/v) PLGA/dioxane/water mixtures (1,4-dioxane/water, 87/13) at the same coarsening temperatures (5°C) (quenching depth, 9°C) during different quenching time. Spinodal separation was expected for these systems. As can be seen in

Figure 6, open, large, and regularly porous structures are observed during the early stage of phase separation (<2 h). Generally, after a short time, phase separation entered the coarsening process during which the thermodynamic driving force comes from minimizing the interfacial tension. The foams prepared by coarsening for 2 and 4 h have similar morphology, and the former shows relatively uniform pores ranging from 30 to 180 μm while the latter indicates irregular pores ranging from 50 to 250 μm. Both of them are macroporous and interconnected. But the foams prepared by quenching for 8 h show very different microstructure from the twos. In the surface, it has many big pores with size at about 200–800 μm, which contain lots of small open pores. This structure may be due to coarsening process occurring via a coalescence mechanism in which larger porous structure are produced by the combination of smaller structure [32].

Data plotted in Figure 7 shows the SEM micrographs of PLGA/NHA foam prepared from 10% (w/v) PLGA/NHA/dioxane/water mixtures (1,4-dioxane/water, 87/13) at different quenching temperatures. Even though the PLGA/NHA solution quenching at 5°C has larger driving force for phase separation, the scaffold made from it shows irregular and small pores.

Effect of NHA Content

The effects of NHA content on the structure of PLGA/NHA foams also have been investigated by varying the NHA amount in the PLGA/NHA foams while maintaining the PLGA concentration constant. Scanning election micros image shows that the microscope structure of the foam changes considerably with the NHA content (Figure 8). Figure 8 shows

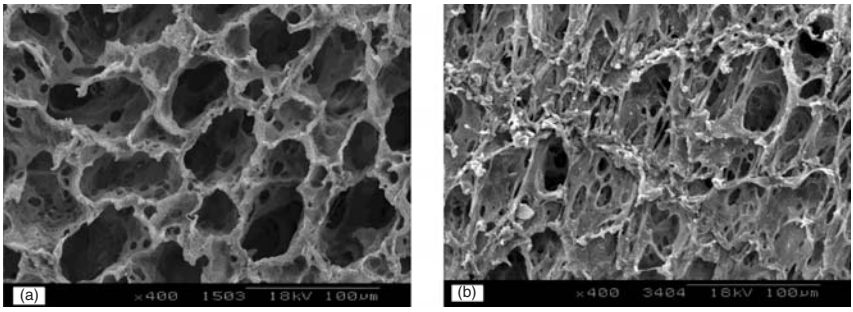

Figure 7. SEM micrographs of PLGA/NHA (PLGA/NHA, 95/5) scaffolds prepared from 10% (w/v) PLGA/NHA/dioxane/water mixtures (1,4-dioxane/water, 87/13) by different quenching temperatures: (a) 9°C and (b) 5°C.

SEM micrographs of PLGA/NHA scaffolds prepared from 10% (w/v) PLGA/dioxane/water mixtures (1,4-dioxane/water, 87/13) with different NHA content after being coarsened at 9°C for 4 h. When the NHA content is low, regular circular pore structure similar to those in pure PLGA foam are observed, and the pore size is about 50–100 μm in diameter (Figure 8a). Most of the pores are connected with their neighbors and have many small pores on the big pore's wall, which entitles the foam's novel connectivity and makes it more suitable to serve as scaffolds for cells seeding and nutrients transporting in tissue engineering. By increasing the NHA content, the pore structure becomes more and more irregular. When the PLGA/NHA ratio is up to 80 : 20, the pore structure becomes so irregular that very little regular circular pore structure is observed and some of the pores are closed. These results have demonstrated that the pore structure of the PLGA foam can be modified by the incorporation of NHA. This conclusion is consistent with that of Zhang and Ma [33] research. From the above

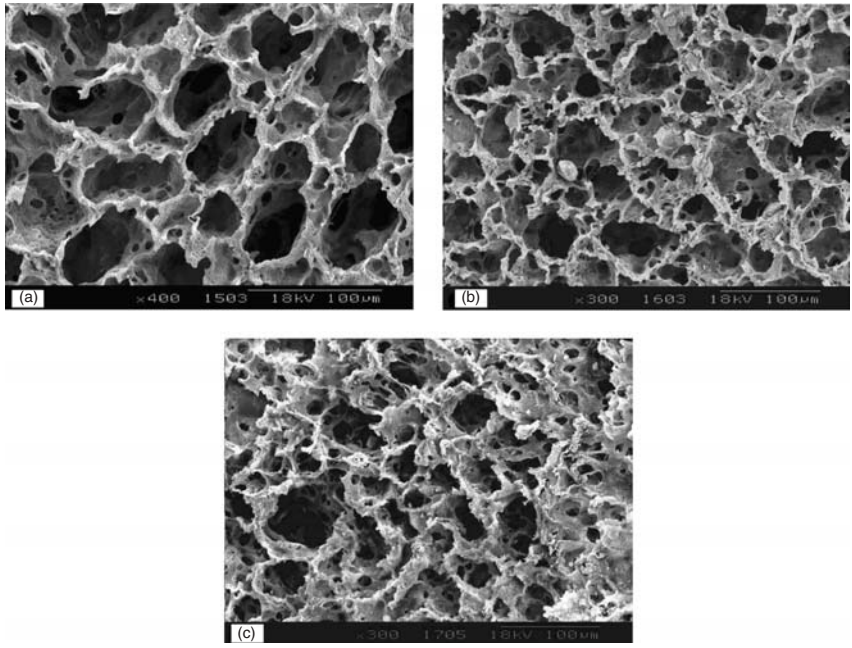

Figure 8. SEM micrographs of PLGA/NHA scaffolds prepared from 10% (w/v) PLGA/dioxane/water mixtures (1,4-dioxane/water, 87/13) with different NHA content after coarsened at 9°C for 4 h: (a) PLGA/NHA, 95/5; (b) PLGA/NHA, 90/10; and (c) PLGA/NHA, 80/20.

conclusion, it is guessed that the porosity of the samples would decrease with the increase of NHA powders, consequently. The porosity of PLGA/NHA scaffolds with different NHA content proves that point (Figure 9).

However, different from the pore size and porosity of the PLGA/NHA scaffold, the water absorption ability and compression strength of PLGA/NHA scaffold increase with the introduction of NHA. As presented in Figure 10, the PLGA/NHA shows improved water absorption ability with the introduction of NHA in the composite scaffolds, while the pure PLGA shows very poor water absorption ability. The enhanced water absorption ability because of the introduction of NHA may be contributed to the interaction between scaffolds and water because of the P-OH groups on the surface of NHA powders. It can be seen from Figure 9 that the scaffolds with NHA take water very rapidly at the very beginning, and the porous structure of the composite scaffolds would make it easy to take in more water.

The NHA content also has a remarkable effect on mechanical properties of the porous scaffolds. Data plotted in Figure 11 suggested that the compression strength of PLGA/NHA scaffolds increases with the increase in NHA contents. The compression strength of PLGA scaffold without NHA is 0.72 MPa, while the compression strength of PLGA scaffold with 25% NHA reaches 2.53 MPa.

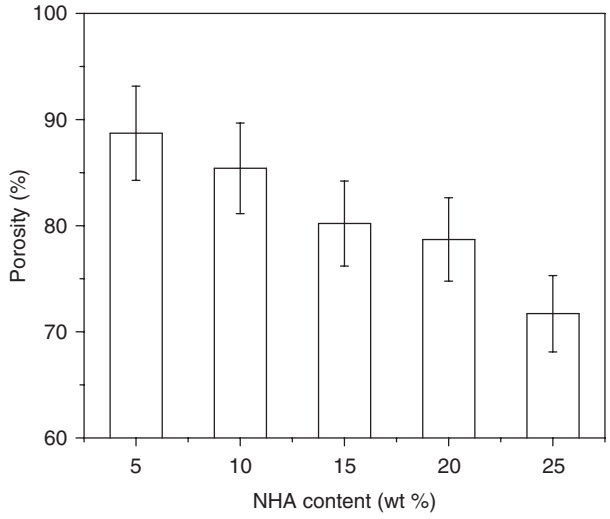

Figure 9. porosity of PLGA/NHA scaffolds prepared from 10% (w/v) PLGA/NHA/dioxane/water mixture (1,4-dioxane/water, 87/13) after being coarsened at 9°C for 4 h with different NHA contents (SD ± 5%).

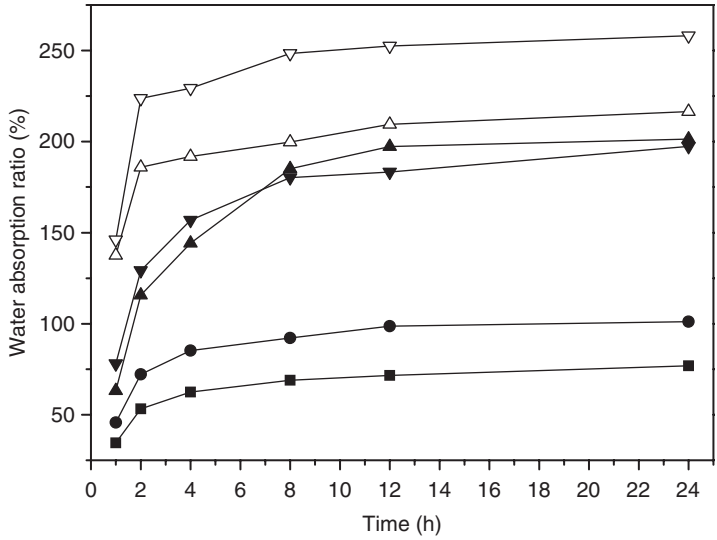

Figure 10. Water absorption ability of PLGA/NHA scaffolds with different NHA contents as a function of soaking time (SD ± 5%). ■ 0 Wt.% ● 5 Wt.% ▲ 10 Wt.% ▼ 15 Wt.% △ 20 Wt.% ▽ 25 Wt.%

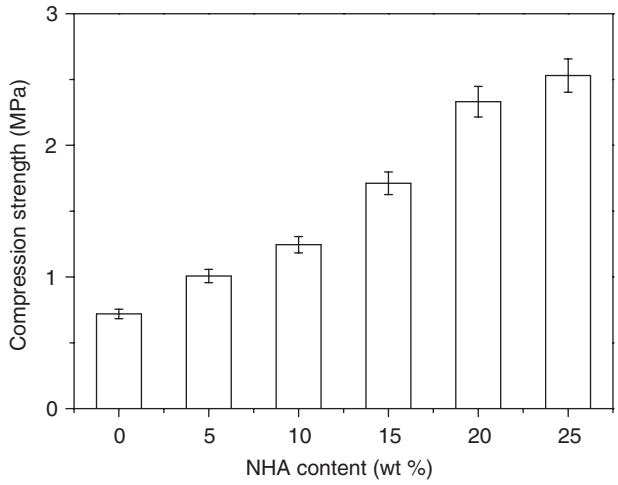

Figure 11. Compression strength of PLGA/NHA scaffolds with different NHA contents (SD ± 5%).

MSCs Culture on PLGA/NHA Scaffolds

In this study, the scaffolds made of PLGA/NHA with various NHA content were investigated for the application as substrates for MSCs. The changes in cell numbers at 3, 5, and 7 days after loading MSCs to the scaffolds were monitored to verify whether MSCs could adhere to and proliferate on the scaffolds or not. The scaffolds used for MSCs seeding are prepared from PLGA, PLGA/NHA (5%), PLGA/NHA (10%) produced by TIPS method with porosity of 91.1, 84.2 (shown in Table 1) and 83.1%, and pore sizes of 100–200 μm shown in Figures 6(a), 8(a), and (b), respectively. The adhesion rate after 4 h in culture and proliferation of the seeded MSCs over the 7-day *in vitro* culture period are shown in Figure 12.

The initial cell seeding density was 1.00×10^6 cells/sample, and the adhesion percentage of PLGA, PLGA/NHA (5%), PLGA/NHA (10%) scaffolds is 34, 38 and 42%, respectively after 4 h in culture, as shown in Figure 12(a). Osteoblasts grew more rapidly in the PLGA/NHA scaffolds than in the PLGA scaffolds without NHA during the 1-week culture period. Three days later, the cell numbers grown on PLGA/NHA (5%) and PLGA/NHA (10%) scaffolds reached 2.10×10^6 and 2.20×10^6, and showed no significant difference between the two scaffolds, but they showed significant difference from the PLGA scaffold without NHA on which 1.80×10^6 cells were grown on. Five days later, the cell numbers grown on PLGA/NHA (5%) and PLGA/NHA (10%) scaffolds reached 4.36×10^6 and 4.52×10^6 and showed no significant difference between the two scaffolds. However, seven days later, the cell numbers grown on PLGA/NHA (5%) and PLGA/NHA (10%) scaffolds reached 6.98×10^6 and 7.31×10^6 and showed significant difference between the two scaffolds. The cell numbers grown on the PLGA/NHA scaffold showed great significant difference from the cell numbers grown on the PLGA scaffolds without NHA.

Alkaline Phosphatase Activity (ALP)

In this study, the optical density (OD), reflecting the total activity of ALP in cells is shown as a function of culture time of cells seeded on the scaffolds; an increase of OD indicates cell adhesion and proliferation in the scaffold. The ALP activity (see Figure 13) of the osteoblasts cultured on PLGA and PLGA/NHA (5%, 10%) scaffolds increased during the 2-week culture period. Three days later, the ALP of osteoblasts grown on the three kinds of scaffolds did not show significant difference. Seven days later, the osteoblass on the PLGA/NHA (5%, 10%) scaffolds showed

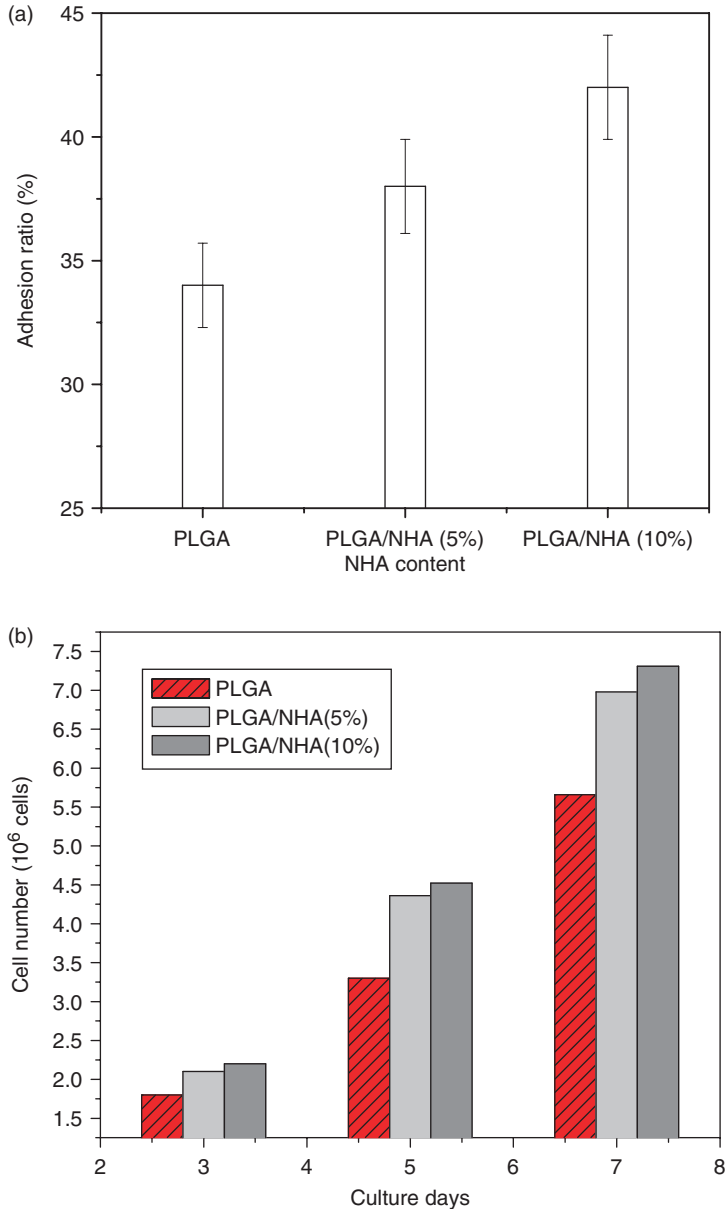

Figure 12. (a) The adhesion rate of MSCs on the PLGA/NHA scaffolds after seeding for 4 h and (b) The number of MSCs attached in the PLGA/NHA scaffolds as a function of time.

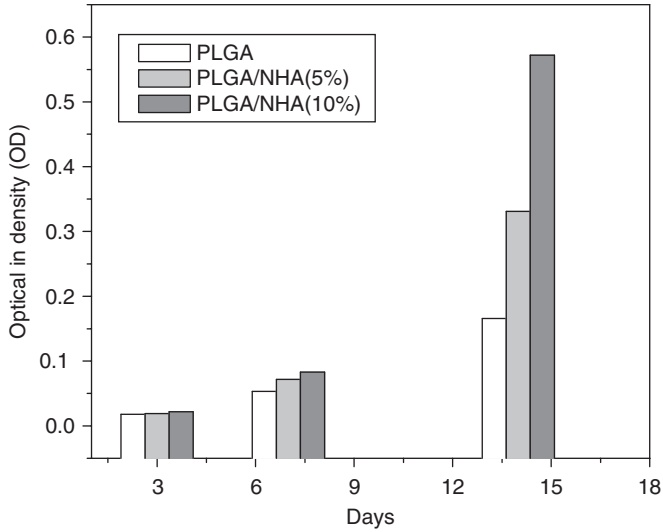

Figure 13. The (ALP) activity of the osteoblasts cultured on PLGA/NHA composite porous scaffolds.

significant higher ($p<0.05$) levels of ALP activity compared to the osteoblasts on the PLGA scaffold without NHA. However, 14 days later, the osteoblasts on the PLGA/NHA (5%) scaffold showed very significant difference from the osteoblasts on the PLGA scaffold without NHA, and the osteoblasts on the PLGA/NHA (10%) scaffolds showed significant difference. The osteoblasts on both PLGA/NHA (5%) and PLGA/NHA (10%) scaffolds showed no significant difference in the first week but showed significant difference in the second week.

Cell Morphology

Round discs were cut from thick cylindrical scaffolds, and MSCs were used to examine the effects of cell behaviors in the scaffolds obtained from our fabrication method. Figure 14 shows ESEM images of the cells cultured for 4 days on the interior surfaces of the scaffold. Control MSCs exhibited a fibroblastic morphology with spindle cell bodies morphologically. After 4 days induction, cells became pyknic, projecting pseudopods into the micropores of PLGA/NHA scaffolds. It is very interesting to see that the MSCs cultured on the PLGA/NHA scaffold had undergone some degree of proliferation and fully covered the inner surface of the PLGA/NHA scaffold. The MSCs/scaffold composite offers a promising approach to restore the bone.

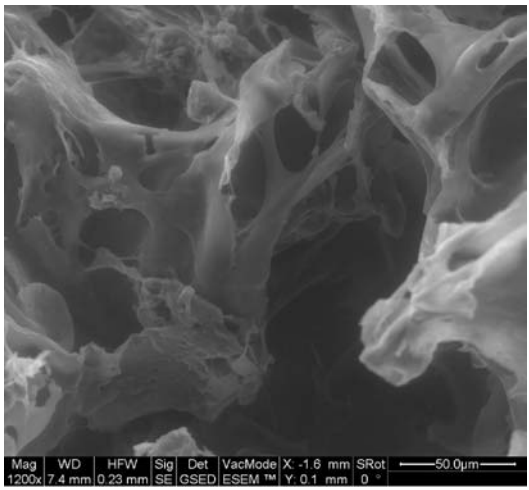

Figure 14. ESEM micrographs of cell proliferation in PLGA/NHA (10%) scaffolds.

DISCUSSION

The present studies described a phase separation technique to fabricate PLGA/NHA composite scaffolds with high porosity and controlled pore architecture and the MSCs were cultured on these scaffolds.

The ultimate porous morphology of a scaffold, including pore size, pore shape, and porosity, is determined by the thermodynamic state of the solution prior to freeze-drying. Phase separation is induced by bimodal or spinodal decomposition on the basis of the location of the system in the miscibility gap in the phase diagram. In this article, different solvent systems were used to obtain scaffolds with different microstructures and properties. When mixed solvent (1,4-dioxane/water) was used to prepare PLGA solutions, a liquid–liquid phase separation was induced and this process dominated the final pore structure of the system [34], resulting in interconnected pore architecture. Although Nam and Park [35] indicated that with the increase of water content in system, larger quenching depth allowed the system to continue on the coarsening process to further reduce the interfacial free energy between two phases separated in earlier stage, which may result in larger pores for scaffold made from phase separation; the results in this article does not seem to be consistent with it. In contrast, consistent with the results of Hua et al.'s [32] research, increasing the water content in the solvent caused the sedimentation boundary to shift to higher polymer concentration which have high viscosity hindering phase separation.

So the PLGA scaffold prepared from PLGA solution (85/15 mixed solvent) with high viscosity shows irregular and small pores. In addition, PLGA solution (85/15 mixed solvent) has to be coarsened at 28°C in order to prevent the formation of polymer gel due to the partial crystallization of PLGA at low temperature.

The polymer concentration has great effect on the morphology of scaffold. As mentioned earlier, the pore size of the obtained scaffolds are related directly to the sizes of the diluent droplets, which coalesce with each other and integrate into bigger droplet by Brownian motion in coarsening process. According to Binder–Stauffer (BS) mechanism [36], which is the widely used theory on the droplet coarsening behavior so far, the mean radius R of the new droplet formed through collision and coalescence is a function of the cubic root of the viscosity of the solution η.

$$R^3 = k^{\mathrm{d}}\left(\frac{k^{\mathrm{B}}T}{5\pi\eta}\right)t \tag{2}$$

where T is the temperature, η is the viscosity, k_{B} is Boltzmann's constant and k_{d} is a constant ($k_{\mathrm{d}} = 6\Phi_{\mathrm{d}}\Phi_{\mathrm{d}}$ is the volume fraction of the minority phase). Therefore, the droplet size is affected by the viscosity of the PLGA solution and decreased when the polymer concentration increases from 8 to 10 wt.%.

The results can be explained as follows: with the concentration of PLGA solution increased, the viscosity of the PLGA/NHA solution is also increased, which hinders the chains' motion of the polymer and increases its viscosity indirectly. Also the NHA particles disturb and obstruct the collision and coalescence of the droplets of diluents, and hence reduces the pore sizes of the sample prepared. This indicates that the droplets of the diluents grow up as a function of coarsening time. As the system is aged at preset temperature, small droplets gradually increase in size. This is also consistent with function (2).

Coarsening temperature has double-faced effects on the products' microstructure (Figure 7). On the one hand, the low viscosity caused by high temperature or low polymer concentration promotes the collision and coalescence of droplets, and hence increases the pore size. On the other hand, the final porous morphology of the scaffold also depends on the thermodynamic state of the solution and the kinetic control, while the thermodynamic driving force for phase separation at a particular PLGA concentration and 1,4-dioxane/water composition is dominated by the quenching depth (the temperature difference between cloud-point temperature and coarsening temperature). So, in this aspect, the lower

the temperature is, the stronger the driving force will be, and the phase separation will occur more early and effectively, which increases the pore sizes consequently. In conclusion, these two kinds of effects have competitive influence on the final structure and morphology of the scaffolds made from phase separation. That is why the PLGA/NHA solution quenching at 5°C has larger driving force for phase separation, while the scaffold made from it shows irregular and small pores. It's the competitive results of the two factors mentioned earlier.

The cloud-point of 10 wt.% PLGA solution in 1,4-dioxane/water (87/13 by weight) is 19°C as shown in Figure 2. The 5°C coarsening temperature gives rise to 14°C quenching depth, while the 9°C one causes a 10°C one. It seems that the former will result in bigger pores with more powerful thermodynamic driving force than the other. But it is the latter that has an irregular and interconnected microstructure in fact. This indicates that the viscosities of the polymer solution dominate the morphology of final products in PLGA/NHA system, when the polymer concentration is relatively high and coarsening temperature is relatively low. The NHA powders added into the solution also greatly affects the integration of diluent droplets by the Brownian motion in the coarsening process. And the morphology development during phase separation under this thermodynamic driving force can be controlled by adjusting the coarsening time.

Enhanced cell culture on the PLGA/NHA scaffolds may result from the direct contact of seeded cells with the NHA particles exposed on the scaffold surface, which stimulate the cell proliferation and osteogenic differentiation [37,38]. The ALP activity on the PLGA scaffold without NHA showed slight changes during the culture period *in vitro*, while the ALP activity on the PLGA/NHA scaffolds displayed significant changes during the 2-week culture period, which may be due to the fact that ALP is an early marker for osteogenic differentiation and usually peaks early. After seeded for 4 days, MSCs cultured on the PLGA/NHA scaffold had undergone some degree of proliferation and fully covered the inner surface of the PLGA/NHA scaffold.

CONCLUSIONS

Regular and highly interconnected macroporous (100–150 μm) PLGA/NHA scaffolds was prepared by TIPS techniques. The influence of solvent composition, polymer concentration, coarsening temperature, and time as well as NHA content on microstructure and properties of the composite scaffolds prepared was studied. A series of characteristic interconnected open pore microstructures with pore sizes ranging from

several microns to a few hundred microns were created. The pore size of the PLGA/NHA scaffolds decreases with the increase of PLGA concentration and HA content. The mechanical properties and water absorption ability of the composite scaffolds are enhanced greatly because of the introduction of NHA. PLGA/NHA scaffolds exhibited significantly higher cell growth, alkaline phosphatase activity than PLGA scaffolds, especially the PLGA/NHA scaffolds with 10 wt.% NHA. These results suggest that the newly developed PLGA/NHA composite scaffolds may serve as an excellent 3D substrate for cell attachment and migration in bone tissue engineering.

ACKNOWLEDGMENTS

The project was sponsored by the key basic research foundation for development of science and technology in Shanghai, P. R. of China (No. 05DJ14006), the Track Plan Project of Rising Star for Youthful Scholar of Shanghai (No. 04QMH1406) and the research foundation for nano-science and technology special project of Shanghai (No. 0452nm088).

REFERENCES

1. Coombes, A.G. and Meikle, M.C. (2004). Resorbable Synthetic Polymers as Replacements for Bone Graft, *Clin. Mater.*, **17**: 35–67.
2. Kim, S.S., Park, M.S., Jeon, O., Choi, C.Y. and Kim, B.S. (2006). Poly(lactide-co-glycolide)/Hydroxyapatite Composite Scaffolds for Bone Tissue Engineering, *Biomaterials*, **27**: 1399–1409.
3. Laurencin, C.T., Attawia, M. and Borden, M.D. (1999). Advancements in Tissue Engineered Bone Substitutes, *Curr. Opin. Orthop.*, **10**: 445–451.
4. Bagambisa, F.B., Joos, U. and Schilli, W. (1993). Mechanisms and Structure of the Bond between Bone and Hydroxyapatite Ceramics, *J. Biomed. Mater. Res.*, **27**(8): 1047–1055.
5. Rizzi, S.C., Heath, D.J., Coombes, A.G., Bock, N., Textor, M. and Downes, S. (2001). Biodegradable Polymer/Hydroxyapatite Composites: Surface Analysis and Initial Attachment of Human Osteoblasts, *J. Biomed. Mater. Res.*, **55**: 475–486.
6. Wang, M. (2003). Developing Bioactive Composite Materials for Tissue Replacement, *Biomaterials*, **24**: 2133–2151.
7. Van, L.P., Li, F., Keustermans, J.P., Streydio, J.M., Delannay, F. and Munting, E. (1995). The Influence of High Sintering Temperatures on the Mechanical Properties of Hydroxyapatite, *J. Mater. Sci. Mater. Med.*, **6**: 8–13.
8. Du, C., Cui, F.Z., Zhu, X.D. and de Groot, K. (1999). Three-dimensional Nano-HAp/Collagen Matrix Loading with Osteogenic Cells in Organ Culture, *J. Biomed. Mater. Res.*, **44**: 407–415.

9. Du, C., Cui, F.Z., Feng, Q.L., Zhu, X.D. and de Groot, K. (1998). Tissue Response to Nano-Hydroxyapatite/Collagen Composite Implants in Marrow Cavity, *J. Biomed. Mater. Res.*, **42**: 540–548.
10. Webster, T.J., Ergun, C., Doremus, R.H., Siegel, R.W. and Bizios, R. (2000). Specific Proteins Mediate Enhanced Osteoblast Adhesion on Nanophase Ceramics, *J. Biomed. Mater. Res.*, **51**: 475–483.
11. Webster, T.J., Siegel, R.W. and Bizios, R. (1999). Osteoblast Adhesion on Nanophase Ceramics, *Biomaterials*, **20**: 1221–1227.
12. Kulkarni, R.K., Pani, K.C. and Neuman, C. (1966). Poly(lactic acid) for Surgical Implants, *Arch. Surg.*, **93**(6): 839–843.
13. Cutright, D.E. and Hunsuck, E.E. (1971). Tissue Reaction to the Biodegradable Poly Lactic Acid Suture, *Oral Surgery*, *Oral Medicine*, *Oral Pathology*, **31**(2): 134–139.
14. Hollinger, J.O. and Battistone, G.C. (1986). Biodegradable Bone Repair Materials: Synthetic Polymers and Ceramics, *Clinical Orthopaedics and Related Research*, **207**: 290–305.
15. Bostman, O.M. (1991). Absorbable Implants for the Fixation of Fractures, *J. Bone Joint Surg.-Am.*, **73A**(1): 148–153.
16. Cordewener, F.W., Bos, R.R. and Rozema, F.R. (1996). Poly(L-lactide) Implants for Repair of Human Orbital Floor Defects: Clinical and Magnetic Resonance Imaging Evaluation of Long-Term Results, *J. Oral Maxillofac. Surg.*, **54**(1): 9–13.
17. Bos, R.R.M., Rozema, F.B., Boering, G., Nijenhius, A.J., Pennings, A.J., Verwey, A.B., Nieuwenhuis, P. and Jansen, H.W.B. (1991). Degradation of and Tissue Reaction to Biodegradable Poly(l-lactide) for Use as Internal Fixation of Fractures: A Study in Rats, *Biomaterials*, **12**(1): 32–36.
18. Tormala, P., Vaiionpaa, S., Kilpikari, J. and Rokkanen P. (1987). The Effects of Fiber Reinforcement and Gold Plating on the Flexual and Tensile Strength of PGA/PLA Copolymer Materials In Vitro, *Biomaterials*, **8**(1): 42–45.
19. Zhang, R. and Ma, P.X. (1999). Porous Poly(L-lactic acid)/Apatite Composites Created by Biomimetic Process, *J. Biomed. Mater. Res.*, **45**: 285–293.
20. Zhang, R. and Ma, P.X. (1999). Poly(alpha-hydroxyl acids)/Hydroxyapatite Porous Composites for Bone Tissue Engineering. I. Preparation and Morphology, *J. Biomed. Mater. Res.*, **44**: 446–455.
21. Thomson, R.C., Yaszemski, M.J., Powers, J.M. and Mikos, A.G. (1998). Hydroxyapatite Fiber Reinforced Poly(alpha-hydroxy ester) Foams for Bone Regeneration, *Biomaterials*, **19**: 1935–1943.
22. Ishaug, S.L., Crane, G.M., Miller, M.J., Yasko, A.W., Yaszemski, M.J. and Mikos, A.G. (1997). Bone Formation by Three-Dimensional Stromal Osteoblast Culture in Biodegradable Polymer Scaffolds, *J. Biomed. Mater. Res.*, **36**: 17–28.
23. Ma, P.X., Zhang, R., Xiao, G. and Franceschi, R. (2001). Engineering New Bone Tissue In Vitro on Highly Porous Poly(Alpha-Hydroxyl Acids)/Hydroxyapatite Composite Scaffolds, *J. Biomed. Mater. Res.*, **54**: 284–293.

24. Mikos, A.G., Lyman, M.D., Freed L.E. and Langer, R. (1994). Wetting of Poly(L-Lactic Acid) and Poly(D,L-Lactic-Co-Glycolic Acid) Foams for Tissue Culture, *Biomaterials*, **15**: 55–58.
25. Mikos, A.G., Sarakinos, G., Vacanti, J.P., Langer, R.S. and Cima, L.G. (1996). Biocompatible Polymer Membranes and Methods of Preparation of Three Dimensional Membrane Structures, US Patent No. 5514378.
26. De Groot, J.H., Kuijper, H.W. and Pennings, A.J. (1997). A Novel Method for Fabrication of Biodegradable Scaffolds with High Compression Moduli, *J. Mater Sci.: Mater. Med.*, **8**: 707–712.
27. Mooney, D.J., Baldwin, D.F., Suh, N.P., Vacanti, J.P. and Langer, R. (1996). Novel Approach to Fabricate Porous Sponges of Poly(D,L-Lactic-Co-Glycolic acid) without the Use of Organic Solvents, *Biomaterials*, **17**(14): 1417–1422.
28. Wang, K., Tomas, C.H. and Healy, K.E. (1995). A Novel Method to Fabricate Bioabsorbable Scaffolds, *Polymer*, **36**: 837–842.
29. Nam, Y.S. and Park, T.G. (1999). Biodegradable Polymeric Microcellular Foams by Modified Thermally Induced Phase Separation Method, *Biomaterials*, **20**: 1783–1790.
30. Ma Peter, X. and Zhang, R.Y. (1999). Synthetic Nano-Scale Fibrous Extra Cellular Matrix, *J. Biomedi. Mater. Res.*, **46**: 60–72.
31. Solchaga, L.A., Johnstone, B., Yoo, J.U., Goldberg, V.M. and Caplan, A.I. (1999). High Variability in Rabbit Bone Marrow-Derived Mesenchymal Cell Preparations, *Cell Transplant*, **8**: 511–519.
32. Hua, F.J., Park, T.G. and Lee, D.S. (2003). A Facile Preparation of Highly Interconnected Macroporous Poly(D,L-Lactic Acid-Co-Glycolic Acid) (PLGA) Scaffold by Liquid-Liquid Phase Separation of a PLGA-Dioxane-Water Ternary System, *Polymer*, **44**: 1911–1920.
33. Zhang, R.Y. and Ma, P.X. (1999). Poly(α-Hydroxyl Acids)/Hydroxyapatite Porous Composites for Bone-Tissue Engineering. I. Preparation and Morphology, *J. Biomedi. Mater. Res.*, **44**: 446–455.
34. Zhang, R.Y. and Ma, P.X. (2001). Processing of Polymer Scaffolds: Phase Separation, In: Atala, A. and Lanza, R. (eds), *Methods of Tissue Engineering*, pp. 715–724, Academic Press, San Diego, CA.
35. Nam, Y.S. and Park, T.G. (1999). Porous Biodegradable Polymeric Scaffolds Prepared by Thermally Induced Phase Separation, *J. Biomed. Mater. Res.*, **47**: 8–17.
36. Binder, K. and Stauffer, D. (1974). Theory for the Slowing Down of the Relaxation and Spino dal Decomposition of Binary Mixtures, *Physical Review Letters*, **33**: 1006–1009.
37. Ambrosio, A.M., Sahota, J.S., Khan, Y. and Laurencin, C.T. (2001). A Novel Amorphous Calcium Phosphate Polymer Ceramic for Bone Repair: I. Synthesis and Characterization, *J. Biomed. Mater. Res.*, **58**: 295–301.
38. Marra, K.G., Szem, J.W., Kumta, P.N., DiMilla, P.A. and Weiss, L.E. (1999). In Vitro Analysis of Biodegradable Polymer Blend/Hydroxyapatite Composites for Bone Tissue Engineering, *J. Biomed. Mater. Res.*, **47**: 324–335.